Numerical Modeling of Gaseous Expansion from Micro and Nano Nozzles

Ryan E. Chamberlin and Nikolaos A. Gatsonis

Mechanical Engineering Department, Worcester Polytechnic Institute, Worcester, MA 01609, USA

Abstract. The expansion of helium from micronozzles into vacuum has been extensively investigated using a three dimensional unstructured DSMC code. Investigations into the effect of Reynolds number, Knudsen number, speed ratio and scale have been carried out. From the comparisons it has been found that the plume profile narrows as both the Knudsen number and speed ratio are increased for a fixed Reynolds number. The relative drop in the number density along the flow path was found to decrease with increasing Knudsen number and speed ratio for a fixed Reynolds number. A slight narrowing of the plume was seen as both the Reynolds number and speed ratio were increased for a fixed Knudsen number. While the relative drop in the number density along the flow path was seen to clearly decrease with increasing Reynolds number and speed ratio for a fixed Knudsen number. It was further observed that the plume profile was not significantly altered when increasing the Knudsen number while decreasing the Reynolds number for a fixed inlet speed ratio.

Keywords: DSMC, micronozzle, nanonozzle, plume
PACS:51.10

INTRODUCTION

The interdisciplinary advancement of the miniaturization movement has impacted nearly every field of technology and science. One such field that has eagerly embraced MEMS and NEMS development is that of satellite propulsion. To date many MEMS based systems have been developed for use as station keeping and attitude control thrusters [1, 2].

Although micropropulsion devices can take a variety of forms, one of the simplest possible configurations can be that of cold gas expansion from a nozzle. Due to its fundamental nature, nozzle expansion has been investigated numerically and experimentally in previous studies [3, 4]. Not until recently however has it been necessary to investigate the nature of gaseous expansion from nozzles in detail as pertaining to the expansion from micronozzles. Therefore the work presented here is intended to compliment and extend previous investigations that where limited to nozzles with a throat diameter of a few millimeters or larger. Additionally, this work offers the transitional background needed for investigations of gaseous expansion from nanonozzles.

In the present work, gas expansion from a conical nozzle is studied using the direct simulation Monte Carlo (DSMC) method for throat diameters ranging from 250 μm down to 250 nm. The angular distribution of the resulting plume is captured in detail for each case investigated. Furthermore, simulations are carried out for a range of inlet Knudsen numbers and the effect of inlet speed ratio and inlet Reynolds number on the plume structure is investigated. The effect of scaling the geometry is also examined.

DSMC METHODOLOGY

The DSMC method has been employed exclusively throughout this work to model the expansion of helium from micronozzles and nanonozzles. The method was initially developed in the early 1960's by G.A. Bird [5]. Modifications and additions to the original algorithms aided in increasing the accuracy of the method in the early

developmental stages [6-8]. Over the last two decades DSMC has become widely accepted as the primary method for modeling rarefied gas flows. In recent years further algorithmic refinements have been introduced [9-11] and analytical efforts have been made that lend further credibility to the method [12-15].

The DSMC code utilized in this work is fully three dimensional and is carried out on unstructured tetrahedral meshes [16]. The majority of the underlying algorithms follow the methodology developed by Bird [5]. As such, the intermolecular collision pair selection process follows the no-time-counter (NTC) scheme. The intermolecular potential model used in this work is the variable hard sphere model (VHS). Helium gas is used for all simulations therefore rotational energy modeling is not required. Furthermore, vibrational energy modeling is also neglected due to the low temperatures encountered within this study. The nozzle walls are modeled as fully diffuse with complete accommodation of tangential momentum and energy.

GEOMETRY AND BOUNDARY CONDITIONS

For this preliminary investigation, the chosen nozzle geometry corresponds to that shown in Fig. 1(a). The geometry is fixed for all cases investigated. Each nozzle features a conical half-angle of 20 degrees and an area ratio of 4. The simulation domains used in this study all feature an internal nozzle region, shown on the left side of Fig. 1(a) and the near field plume expansion region, as seen in the right side of Fig. 1(a). Although the grid spacing varies for each case a few relations remain constant amongst all cases. The first relation that is guaranteed for all grids is that the local cell spacing is always smaller than the local mean free path. This is a widely accepted limit that, when coupled with a properly chosen time step and a sufficient number of simulated particles in each cell, ensures physical collision pair spacing and thus statistically accurate modeling of transport phenomena [14, 15]. The second cell spacing criteria common to all grids is sizing bounded by geometric resolution. In certain cases investigated in this work the local mean free path is much larger than that the nozzle throat diameter. When this relation holds the cell spacing is set to the maximum size that still leads to a sufficient capturing of the nozzle curvature. An example of the unstructured grids used in the nozzle simulations is shown in Fig. 1(b).

Within the cases studied here, the particle injection along the inlet of the nozzle is modeled as a molecular flux of an equilibrium gas. As such, the pressure, temperature and drift velocity of the equilibrium distribution at the boundary are chosen at initialization and enforced throughout the simulation. To aid in the development of a corresponding equilibrium distribution in the region of the inlet surface at steady state, any particles that move upstream along the inlet surface are removed from the flow. Although this method constrains the flow properties at the inlet, and thus does not allow for a floating drift velocity as is needed for standard subsonic boundary conditions, the inlet constraints are still physical and are appropriate for modeling the entrance region of an arbitrary flow field. Furthermore, the inlet flow constraints allow for simple manipulation of the inlet Knudsen number and Reynolds number as is required for the investigation at hand.

The walls of the nozzle are modeled as fully diffuse and the temperature of the wall is chosen to equal that of the inlet distribution. To keep the results as general as possible a hard vacuum was chosen to model the boundaries of the plume region. Although a backpressure boundary condition would be a better match for experimental investigation, the minimum achievable backpressure for each case investigated would vary with each facility. However, future investigations are planned which will study the effect of backpressure on the plume properties.

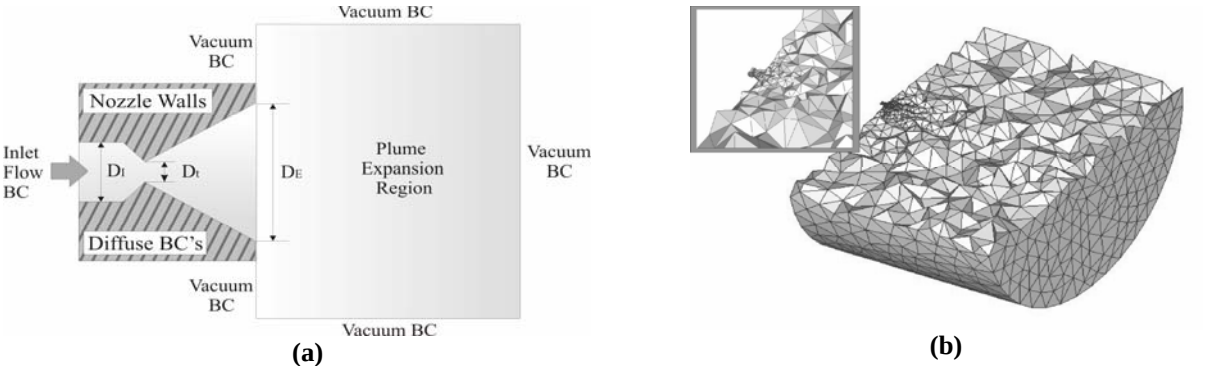

FIGURE 1. Geometry and boundary conditions used in the nozzle simulations **(a).** An example of the unstructured grids used in the nozzle simulations, illustrating the localized grid spacing **(b)**.

It should be noted that for small Reynolds number flows DSMC results exhibit significant numerical scatter. Furthermore statistical uncertainty is known to be large for small Reynolds numbers and speed ratios [17]. In order to reduce the statistical error in the results shown here, extensive time averaging of the data has been carried out for each case studied. Additionally, the number of simulation particles in each computational collision cell is maintained at well over twenty, while macroscopic parameters are calculated over volumes featuring at least 100 simulation particles. Although the computational cost of these features is considerable the statistical error and random noise in the resulting data is drastically reduced, even using standard DSMC implementation.

RESULTS AND DISCUSSION

The focus of this study is to identify the key parameters governing the expansion of gas from miconozzles and nanonozzles. A secondary goal of this work is to characterize the effects of each key parameter on the resulting plume structure. The parameters under consideration for this study are the inlet Knudsen number (Kn), Reynolds number (Re) and speed ratio (S). The definitions used within this work were derived for the VHS model and take the form [5]:

$$\mathrm{Kn} = \frac{\lambda}{\mathrm{D}} = \frac{1}{\sqrt{2}\pi \mathrm{d_{ref}}^2 \mathrm{n}\left(\mathrm{T_{ref}}/\mathrm{T}\right)^{\omega-1/2}} \frac{1}{\mathrm{D}} \tag{1}$$

$$\mathrm{Re} = \frac{2(5-2\omega)(7-2\omega)}{15\pi} \frac{\mathrm{S}}{\mathrm{Kn}} \tag{2}$$

$$\mathrm{S} = \frac{\mathrm{V}}{\sqrt{2\mathrm{kT}/\mathrm{m}}} \tag{3}$$

For the purpose of identifying and characterizing the effects of the key parameters a parametric study has been carried out over a range of parameter values. The resulting plume profiles are compared for each parameter set.

The first parameter set under investigation is chosen such that each case shares a common inlet Reynolds number of 0.5. When using the VHS definitions, varying the Knudsen number while fixing the Reynolds number requires that the speed ratio also varies. Unfortunately the relation between the commonly used governing parameters undermines the isolation of each potential key parameter. However, by carrying out several parameter set comparisons with each potential key parameter fixed one can gain insight into the significance of each parameter.

TABLE 1. Parameter values used for fixed Reynolds number (Re) simulations.

	$\mathbf{D_t}$ (μm)	$\mathbf{n_I}$ ($\mathbf{m^{-3}}$)	V (m/s)	T (K)	Re	Kn	S
Case 1	250	1.65e23	35	300	0.5	0.1	0.03
Case 2	250	1.65e22	350	300	0.5	1	0.3
Case 3	250	1.65e21	3500	300	0.5	10	3

The parameter values used for the first set of simulations are given in Table 1. For the purpose of the current study, the number density is sampled as a function of the radial distance from the nozzle exit plane as well as the angle from the nozzle axis, $\mathbf{n(R,\theta)}$. The resulting plume profiles are seen in Fig. 2. Figure 2(a) is a comparison plot of the number density, normalized by the centerline value $\mathbf{n_0 = n(R,0)}$, at a radial distance of 20 exit diameters (40 throat diameters). From the comparison plot of Fig. 2(a) a clear narrowing of the plume can be seen as both the Knudsen number and speed ratio are increased. Figure 2(b) is a comparison plot of the number density, also at a radial distance of 20 exit diameters, scaled using the inlet value $\mathbf{n_I = n(x_{Inlet},0)}$. From Fig. 2(b) it can be seen that the relative drop in the number density along the flow path decreases with increasing Knudsen number and speed ratio.

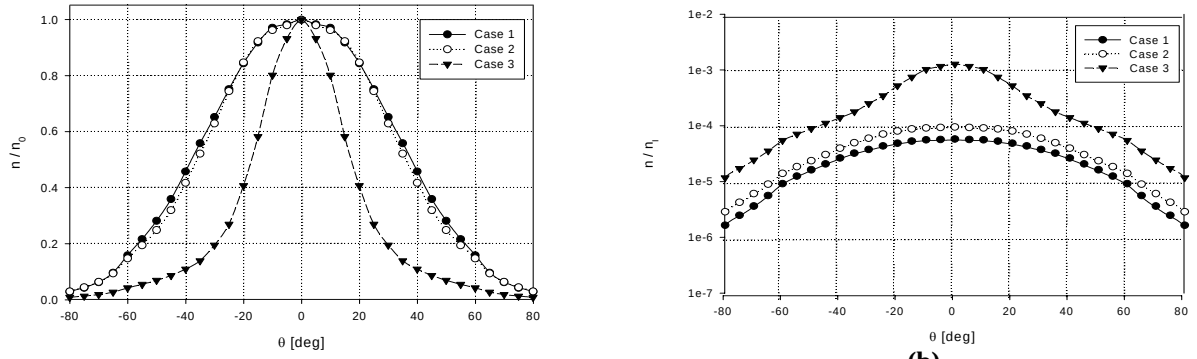

(a) **(b)**

FIGURE 2. Plume profiles for parameter sets with a common inlet Reynolds number of 0.5, sampled at a radial distance of 40 throat diameters from the nozzle exit plane.

The second parameter set investigated is chosen such that each case shares a common inlet Knudsen number. The chosen value for the common Knudsen number is 1, which is well within the transitional regime. The parameter values used for the second set of simulations are given in Table 2.

TABLE 2. Parameter values used for fixed Knudsen number (Kn) simulations.

	D_t (μm)	n_I (m^{-3})	V (m/s)	T (K)	Re	Kn	S
Case 4	250	1.65e22	3500	300	5	1	3
Case 5	250	1.65e22	350	300	0.5	1	0.3
Case 6	250	1.65e22	35	300	0.05	1	0.03
Case 7	250	1.65e22	3.5	300	0.005	1	0.003

The resulting plume profiles are seen in Fig. 3. In Fig. 3(a) a slight narrowing of the plume can be seen as both the Reynolds number and speed ratio are increased. From Fig. 3(b) it can be seen that the relative drop in the number density along the flow path clearly decreases with increasing Reynolds number and speed ratio.

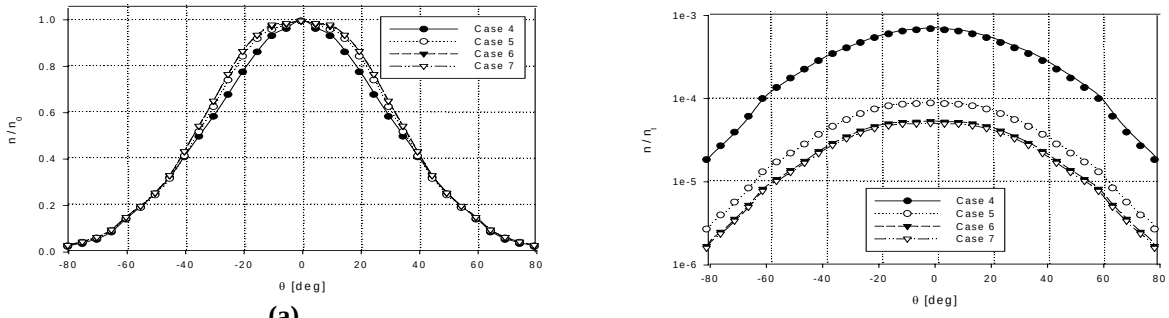

(a) **(b)**

FIGURE 3. Plume profiles for parameter sets with a common inlet Knudsen number of 1, sampled at a radial distance of 40 throat diameters from the nozzle exit plane.

The third parameter set under investigation is chosen such that each case shares a common inlet speed ratio of 0.03. The parameter values used for the third set of simulations are given in Table 3. The resulting plume profiles are seen in Fig. 4.

TABLE 3. Parameter values used for fixed speed ratio (S) simulations.

	D_t (μm)	n_I (m^{-3})	V (m/s)	T (K)	Re	Kn	S
Case 8	250	1.65e23	35	300	0.5	0.1	0.03
Case 9	250	1.65e22	35	300	0.05	1	0.03
Case 10	250	1.65e21	35	300	0.005	10	0.03

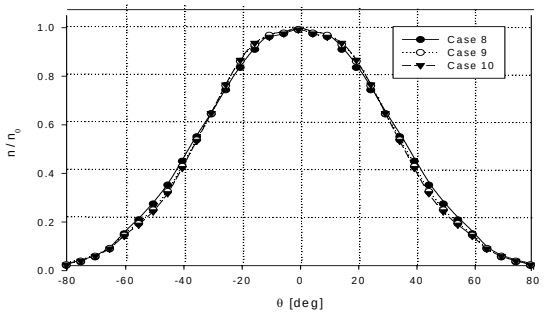

(a)

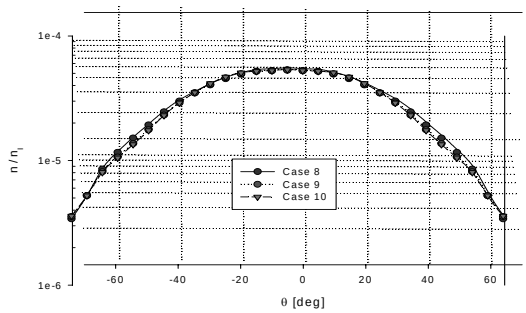

(b)

FIGURE 4. Plume profiles for parameter sets with a common inlet speed ratio of 0.03, sampled at a radial distance of 40 throat diameters from the nozzle exit plane.

In Fig. 4(a) and Fig. 4(b) the comparison plots seem to indicate that the plume profile is not significantly altered by increasing the Knudsen number or decreasing the Reynolds number provided that the speed ratio is fixed. The cause for the fixed plume profile is uncertain but is most likely attributed to one of two possibilities. Either the speed ratio is the dominate parameter effecting the plume structure or the effects incurred as the Knudsen number increases and the Reynolds number decreases cancel each other out. Further study is required to ascertain the cause of the static plume profile seen in this parameter set.

The final data set investigated in this study isolates the effect of nozzle scale on the resulting plume profile predicted by the base DSMC implementation. Two nozzle scales are simulated. The first has a throat diameter of 250 μm while the second has a throat diameter of only 250 nm. For both cases the nozzle geometry is identical as are the values of the inlet Knudsen number, Reynolds number and speed ratio. The simulation parameters are given in Table 4.

TABLE 4. Parameter values used for scale simulations.

	D_t	n_I (m^{-3})	V (m/s)	T (K)	Re	Kn	S
Case 11	250 μm	1.65e22	350	300	0.5	1	0.3
Case 12	250 nm	1.65e25	350	300	0.5	1	0.3

The resulting plume profiles are seen in Fig. 5. In Fig. 5(a) and Fig. 5(b) the comparison plots indicate that the plume profile is not significantly altered by decreasing the nozzle scale provided that the Knudsen number, Reynolds number and speed ratio are fixed. This result is expected considering that the base DSMC implementation is scale insensitive and does not capture the microscopic effects that would become more prevalent at the reduced scales seen here. Figure 5(a) illustrates one effect of reducing the scale of the DSMC simulation domain which is a significant increase in statistical fluctuations in the sampling of macroscopic variables. For the simulation sets shown above the results were obtained using time-averaged data which were averaged over twenty data sets (of 100 iteration intervals) in order to obtain number density data where the statistical noise was reduced to a point where 95% confidence interval error bars were smaller than the plotted point markers. For the nanoscaled nozzle, data averaging was carried out over 100 data sets yet the reduction in the statistical scatter amongst the plotted points is comparatively large. Future work is planned that will lend further insight into the scale-induced increase in statistical scatter in DSMC simulation at the nanoscale.

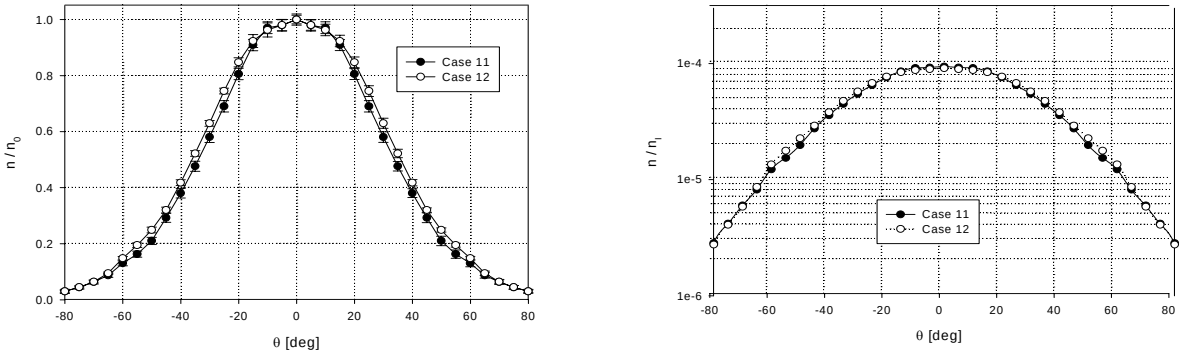

(a) **(b)**

FIGURE 5. Plume profiles for parameter sets with a common inlet speed ratio of 0.03, sampled at a radial distance of 40 throat diameters from the nozzle exit plane.

CONCLUSIONS

A parametric study has been carried out over a range of Knudsen number, Reynolds number and speed ratio values. The resulting plume profiles were compared for each set of parameters. From the comparisons it has been found that the plume profile narrows as both the Knudsen number and speed ratio are increased for a fixed Reynolds number. The relative drop in the number density along the flow path was found to decrease with increasing Knudsen number and speed ratio for a fixed Reynolds number. A slight narrowing of the plume was seen as both the Reynolds number and speed ratio were increased for a fixed Knudsen number. While the relative drop in the number density along the flow path clearly decreases with increasing Reynolds number and speed ratio for a fixed Knudsen number. It was further observed that the plume profile is not significantly altered when increasing the Knudsen number while decreasing the Reynolds number with the speed ratio fixed. With the exception of an increase in statistical fluctuations, the current DSMC implementation has been found to be scale insensitive.

ACKNOWLEDGMENTS

This work was partially supported by NSF's NIRT Program through Grant DMI-0210258 and AFOSR's Computational Mathematics Program through Grant F49620-03-1-0219.

REFERENCES

1. D.H. Lewis, S.W. Janson, R.B. Cohen and E.K. Antonsson, *Sensors and Actuators*, **80**, 143-154 (2000)
2. C. Rossi, S. Orieux, B. Larangot, T. Do Conto and D. Esteve, *Sensor and Actuators A*, **99**, 125-133 (2002)
3. I.D. Boyd, P. F. Penko, D. L. Meissner and K. J. DeWitt, *AIAA Journal*, **30**, 2453-2461 (1992)
4. I.D. Boyd, Y. Jafry and J. Banden Beukel, *Journal of Spacecraft and Rockets*, **31**, 271-277 (1994)
5. G.A. Bird, *Molecular Gas Dynamics and the Direct Simulation of Gas Flows*, Oxford Univ. Press, Oxford, 1996
6. C. Borgnakke, and P.S. Larsen, *J. Comp. Phys.*, **18**, 405-420 (1975)
7. S. Cercignani, and M. Lampis, *Rarefied gas dynamics*, Academic Press, New York, 1974
8. J.A. Lordi, and R.E. Mates, *Phys. Fluids*, **13**, 291-308 (1970)
9. I.D. Boyd, *Phys. Fluids A*, **5**, 2278-2286 (1993)
10. B.L. Haas and I.D. Boyd, *Phys. Fluids A*, **5**, 478-489 (1993)
11. B.L. Haas, D.B. Hash, G.A. Bird, F.E. Lumpkin and H.A. Hassan, *Phys. Fluids A*, **6**, 2191-2201 (1994)
12. S. Rjasanow, and W. Wagner, *Mathematics and Computers in Simulation*, **48**, 151-176 (1998)
13. F.J. Alexander, A.L. Garcia and B.J. Alder, *Phys. Fluids*, **10**, 1540-1542 (1998)
14. A.L. Garcia and W. Wagner, *Phys. Fluids*, **12**, 2621-2633 (2000)
15. N.G. Hadjiconstantinou, *Phys. Fluids*, **12**, 2634-2638 (2000)
16. J. Hammel, K. Kovalev and N.A. Gatsonis, *Proc. of the 35th AIAA Thermophysics Conf.*, Anahiem, CA, June, 2001
17. N.G. Hadjiconstantinou, A.L. Garcia, M.Z. Bazant, and G. He, *J. Comp. Phys.*, **187**, 274-297 (2003)